# EPPLER AIRFOIL DESIGN AND ANALYSIS CODE

## INTRODUCTION

The application of potential-flow theory together with boundary-layer theory to airfoil design and analysis was accomplished many years ago. Since then, potential-flow and boundary-layer theories have been steadily improved. With the advent of computers, these theories have been used increasingly to complement wind-tunnel tests. Today, computing costs are so low that a complete potential-flow and boundary-layer analysis of an airfoil costs considerably less than one percent of the equivalent wind-tunnel test. Accordingly, the tendency today is toward more and more commonly applicable computer codes. These codes reduce the amount of required wind-tunnel testing and allow airfoils to be tailored to each specific application.

The code described in this paper has been developed over the past 45 years. It combines a conformal-mapping method for the design of airfoils with prescribed velocity-distribution characteristics, a panel method for the analysis of the potential flow about given airfoils, and an integral boundary-layer method. It is very efficient and has been successfully applied at Reynolds numbers from $3 \times 10^4$ to $5 \times 10^7$. A compressibility correction to the velocity distributions, which is valid as long as the local flow is not supersonic, has been incorporated into the code. (See refs. 1 and 2.) It is strongly recommended that reference 1 be studied before purchasing the code.

## THEORY

### Potential-Flow Airfoil Design Method

The airfoil design method is based on conformal mapping. This method differs from other inverse methods in that the velocity distribution is not specified at only one angle of attack. Instead, angles of attack that will result in constant velocity over specified segments of the airfoil are input. In other words, pairs of parameters are specified: the segment of the airfoil and the angle of attack relative to the zero-lift line that will result in constant velocity over that segment. Of course, some matching conditions must be met to guarantee a smooth velocity distribution for all angles of attack. Toward the trailing edge, on both surfaces, a main pressure recovery can be specified. Finally, a short closure contribution must be introduced to ensure that the trailing edge will be closed.

In reality, the segments corresponding to the various input angles of attack are not specified in the airfoil plane but rather in the conformal-mapping plane in which the airfoil is represented by a circle. No difficulties have arisen in correlating the arcs of the circle with the segments of the airfoil. An option has been included that allows a transition ramp to be specified by only two points, a forward and an aft limit, relative to the beginning of the pressure recovery.

It should be remembered that for any given velocity distribution there does not necessarily exist a “normal” airfoil. For example, the closure contributions could be quite large, which would result in a very large trailing-edge angle. The closure contributions could also give rise to a region of negative thickness near the trailing edge. Accordingly, several iteration options have been included that allow the trailing-edge angle to be specified while certain input angles of attack or the amount of pressure recovery is iterated.

## Potential-Flow Airfoil Analysis Method

The potential-flow airfoil analysis method employs panels with parabolic vorticity distributions. The geometry of the panels is determined by a spline fit of the airfoil coordinates, with the end points of the panels being the input airfoil coordinates themselves. The flow condition, which requires the inner tangential velocity to be zero, is satisfied at each airfoil coordinate (i.e., at the end points of the panels, not the midpoints). Two angles of attack, 0° and 90°, are analyzed. The flow at an arbitrary angle of attack is derived from these two solutions by superposition. The entire procedure does not require any restrictions on the input point distribution, smoothing, or rearranging of the coordinates; only the original airfoil coordinates are used. An option is included by which additional points can be splined in between the original coordinates. This option allows more precise results to be obtained should a portion of the airfoil have a sparse distribution of points. An option is provided for smoothing airfoils. In addition, several options are available for the generation of coordinates for NACA 4-digit, 5-digit, and 6-series airfoils as well as FX (Wortmann) airfoils.

A flap deflection can be introduced by geometrically rotating part of the airfoil about a flap-hinge point. The connection between the forward portion of the airfoil and the flap is defined by an arc consisting of additional points that are generated automatically according to an input arc length. In addition, an option is included that allows the analysis of chord-increasing flaps. It should be noted that, while the airfoil shape that results from the exercise of this option does have an increased chord, it does not contain a slot and, therefore, is still a single-element as opposed to a multielement airfoil. An option is also provided for analyzing cascades.

## Boundary-Layer Method

The laminar and turbulent boundary-layer development is computed using integral momentum and energy equations. The approximate solutions obtained from the laminar boundary-layer method agree very well with exact solutions. The turbulent boundary-layer method is based on the best available empirical skin-friction, dissipation, and shape-factor laws.

Of special interest are the predictions of separation and transition. The prediction of separation is determined by the shape factor based on energy and momentum thicknesses. (Note that this shape factor has the opposite tendency of the shape factor based on displacement and momentum thicknesses.) For laminar boundary layers, there exists a constant and reliable lower limit of this shape factor, which equals 1.515 and corresponds to laminar separation. For turbulent boundary layers, no such unique and reliable limit exists. It has been determined, however, that the turbulent boundary layer will separate if the shape factor falls below 1.46 and will not separate if the shape factor remains above 1.58. It has also been determined that thicker boundary layers tend to separate at lower shape factors. The uncertainty is not a significant disadvantage because the shape factor changes rapidly near separation. Nevertheless, results must be checked carefully with respect to turbulent separation.

The prediction of transition is based on an empirical criterion that contains the Reynolds number, based on local conditions and momentum thickness, and the shape factor. Previously, the transition criterion used was a local criterion. Recently, a new empirical transition criterion has been implemented that considers the instability history of the boundary layer. The results predicted using the new criterion are comparable to those using the $e^n$ method but the computing time is negligible. The criterion contains a "roughness factor" that allows various degrees of surface roughness or free-stream turbulence to be simulated. The prediction of transition results in a switch from the laminar skin-friction, dissipation, and shape-factor laws to the turbulent ones, without changing the shape factor or the momentum thickness. Also, a procedure has recently been incorporated into the code that empirically estimates the increase in the boundary-layer thickness due to laminar separation bubbles; this procedure yields an additional "bubble drag."

The code contains an option that allows the analysis of the effect of single roughness elements on a turbulent as well as a laminar boundary layer. For the laminar case, transition is assumed to occur at the position of the roughness element. This simulates fixing transition by roughness in a wind tunnel or in flight.

The lift and pitching-moment coefficients are determined from the potential flow. Viscous corrections are then applied to these coefficients. The lift-curve slope where no separation is present is reduced to $2\pi$ from its theoretical value. In other words, the potential-flow thickness effects are assumed to be offset by the boundary-layer displacement effects. A lift-coefficient correction due to separation is also included. As an option, the displacement effect on the velocity distributions and the lift and pitching-moment coefficients can be computed. The boundary-layer characteristics at the trailing edge are used for the calculation of the profile-drag coefficient by a Squire-Young type formula. In general, the theoretical predictions agree well with experimental measurements. (See ref. 3, for example.)

The code contains an option that allows aircraft-oriented boundary-layer developments to be computed, where the Reynolds number and the Mach number vary with aircraft lift coefficient and the local wing chord. In addition, a local twist angle can be input. Aircraft polars that include the induced drag and an aircraft parasite drag can also be computed.

## COMPUTER-SYSTEM CONSIDERATIONS

The code will execute on almost any personal computer (PC), workstation, or server, with run times varying accordingly. The most computationally intensive part of the code, the analysis method, takes only a few seconds to run on a Pentium®-based machine. The boundary-layer method executes more quickly and the design method runs very quickly on all machines.

The code is written in standard FORTRAN77 and, therefore, a FORTRAN compiler is required to translate the supplied source code into executable code. A sample input and output case is included. All the graphics routines are contained in a separate, plot-postprocessing code that is also supplied. The postprocessing code generates an output file that can be sent directly to either a PostScript®-compatible or an HP LaserJet® printer. The user can adapt the postprocessing code to other plotting devices, including the screen. Examples of plots generated by the code follow.

## CONCLUDING REMARKS

This code represents a mathematical model of the two-dimensional viscous flow around airfoils—a computer wind tunnel. The cost of a theoretical analysis of an airfoil is significantly less than the cost of the corresponding wind-tunnel test. Thus, wind tunnels should be employed increasingly to perform investigations concerning fundamental phenomena such as transition and separation. The results from such investigations can then be incorporated into the computer wind tunnel and, thereby, allow airfoils to be theoretically developed for specific applications with increasingly higher degrees of confidence.

## REFERENCES

1. Eppler, Richard: Airfoil Design and Data. Springer-Verlag (Berlin), 1990.

2. Eppler, Richard: Airfoil Program System “PROFIL00.” User’s Guide. Richard Eppler, c.2000.

3. Somers, Dan M.: Subsonic Natural-Laminar-Flow Airfoils. Natural Laminar Flow and Laminar Flow Control, R. W. Barnwell and M. Y. Hussaini, eds., Springer-Verlag New York, Inc., 1992, pp. 143–176.

## AVAILABILITY

The code is available, for a fee, in North America exclusively from:

Dr. Mark D. Maughmer
RR 1, Box 965
Petersburg, PA 16669
USA

and everywhere else from:

Prof. Dr. Richard Eppler
Leibnizstr. 84
D-70193 Stuttgart
GERMANY

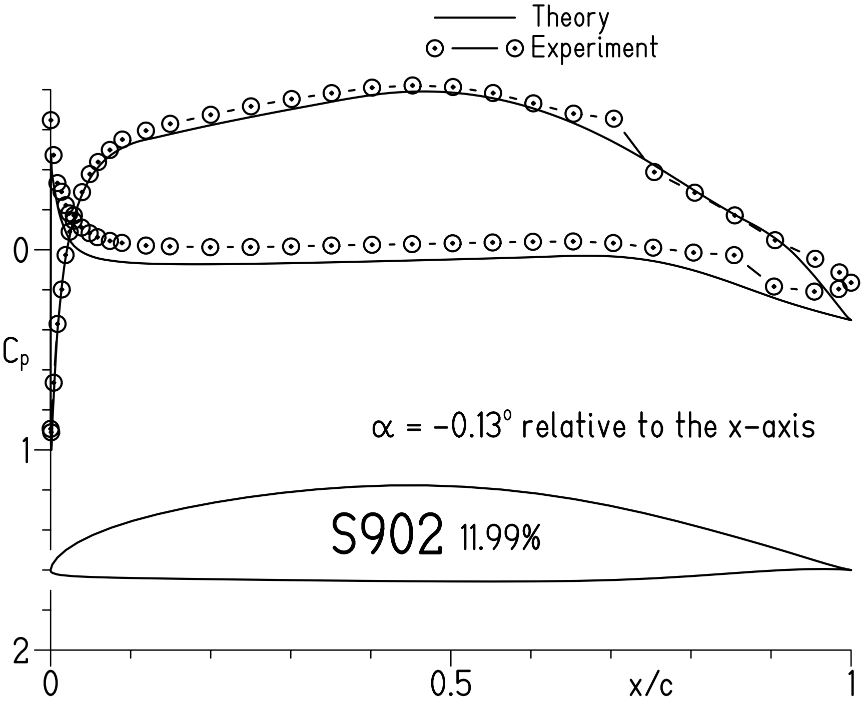
Theory
Experiment
0
C_p
1
2
0
0.5
x/c
1
α = −0.13° relative to the x-axis
S902 11.99%

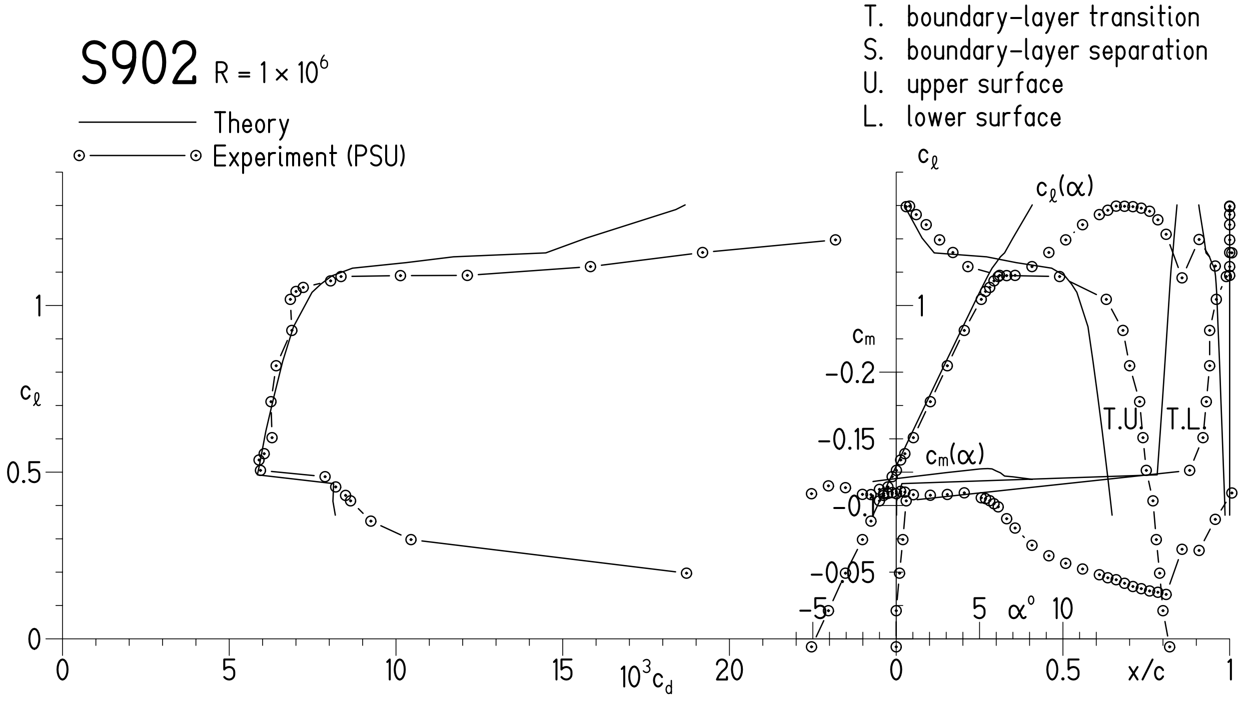
S902 R = 1 × 10^6
Theory
Experiment (PSU)
T. boundary-layer transition
S. boundary-layer separation
U. upper surface
L. lower surface
c_ℓ
1
0.5
0
0
5
10
15
10^3 c_d
20
c_ℓ
c_ℓ(α)
1
c_m
−0.2
−0.15
c_m(α)
−0.1
−0.05
−5
5
α°
10
T.U.
T.L.
0
0.5
x/c
1